Exp Fluids
DOI 10.1007/s00348-007-0269-3

RESEARCH ARTICLE

Detection of microorganismic flows by linear and nonlinear optical methods and automatic correction of erroneous images artefacts and moving boundaries in image generating methods by a neuronumerical hybrid implementing the Taylor's hypothesis as a priori knowledge

Hannes Petermeier · Wojciech Kowalczyk · Antonio Delgado · Cornelia Denz · Frank Holtmann

Received: 27 September 2006 / Revised: 25 January 2007 / Accepted: 26 January 2007

Abstract In biological fluid mechanics powerful imaging methods for flow analysis are required for making progress towards a better understanding of natural phenomena being optimised in the course of evolution. At the same time it is of crucial importance that the measuring and flow visualisation techniques employed guarantee biocompatibility, i.e. they do not distort the behaviour of biosystems. Unfortunately, this restricts seriously the measures for optimising the image generation in comparison to other flow fields in which no biological systems are present. As a consequence, images of lower quality leading to erroneous artefacts are obtained. Thus, either novel detection techniques that are able to overcome these disadvantages or advanced evaluation methods enabling the sophisticated analysis and description of flow fields are essential. In the present contribution, both areas are covered. A novel so-called neuronumerical hybrid allows to detect artefacts in conventional experimental particle image velocimetry (PIV) data of microorganismic flow fields generated by ciliates. The handling of artefacts is performed by the hybrid using a priori knowledge of the flow physics formulated in numerical expressions and the enormous potential of artificial neural networks in predicting artefacts and correcting them. In fact, the neuronumerical hybrid based on the physical knowledge provided by the Taylor's hypothesis can detect not only spurious velocity vectors but also additional phenomena like a moving boundary, in the present case caused by the contraction of the zooid of a microorganism. Apart from the detection of the artefacts, a correction of the spurious velocity vectors is possible. Furthermore, a method to detect microscopic velocity fields based on nonlinear optical filtering, optical novelty filter (ONF) is presented. On the one hand, it can be employed to expose phase changes in flow fields directly from the nonlinear response and without additional tracers. On the other hand, it can be used to preprocess low quality images of flow fields loaded with particles and extract the motion of particles with an enhanced contrast. The flow fields obtained by the correlation based PIV method of the ONF filtered and unfiltered image sequences are compared and discussed.

H. Petermeier (✉)
Informations Technologie Weihenstephan (ITW),
Technische Universität München, Am Forum 1,
85350 Freising, Germany
e-mail: petermeier@wzw.tum.de

W. Kowalczyk · A. Delgado
Lehrstuhl für Strömungsmechanik (LSTM),
Friedrich-Alexander-Universität Erlangen-Nürnberg,
Cauerstrasse 4, 91058 Erlangen, Germany

C. Denz · F. Holtmann
Institut für Angewandte Physik,
Westfälische Wilhelms-Universität Münster,
Corrensstr. 2/4, 48149 Münster, Germany

1 Introduction

Fluid dynamical processes that are observed in nature are supposed to be evolutionarily optimised from the energetical point of view. Thus, at present, significant efforts are performed in order to achieve a better

insight into the principles of minimal energy as employed by biological systems and in transferring them to technical applications. Often, at least a fluid phase or fluid component participates in the energy conversion process or even dominates it. For example, this is a case in aquatic communities, which show an amazing management of their own energy resources in the surrounding water. In fact, the effectiveness of its mechanisms of swimming enables the *Anguilla anguilla* to override more than 5,000 km without ingestion (van Ginneken et al. 2005). Thus, its energy balance demonstrates a clear superiority of natural conversion systems to technical ones.

Unfortunately, often the investigation techniques for analysing appropriately the energy conversion of creatures in fluids which allow accurate studies of the behaviour of the natural system without methodologically caused interceptions are not available. This is the case particularly in microbiological systems which are in the focus of interest of the present contribution. This is especially due to their strong sensitivity to any alteration of the natural milieu. For example, microbes are stressed among other milieu conditions by temperature changes and could be even killed by light radiation. As a consequence, assuring biocompatibility is a basic demand for any measurement technique to be employed.

Here, the convection induced by microorganisms which are member of an aquatic ecosystem is studied. An example of biological systems where many interesting biofluiddynamical processes occur is wastewater purification. In this technique different species of microorganisms cover surfaces like membranes or beads building a biologically active biofilm in order to enable effective mass exchange processes. Such biofilms consist of bacteria and protozoa attaching to the surface and forming an initial layer using an extracellular polymer substance (EPS) network. Initially, individual organisms grow to large colonies (see Fig. 1), which are built among others by ciliates like Vorticella and Opercularia (Foissner et al. 1992). The activity of these species initialises a fluid flow in the biofilm vicinity. This fluid motion is provoked by their ciliary movement. It aims at providing nutrients for themselves and distribution of them in the surrounding area (e.g. Eisenmann et al. 2001).

The experimental observations of Sleigh and Barlow (1976) consider the first flow patterns induced by Vorticella. The authors use latex particles and bacteria *E. coli* for microscopic visualisation of the flow. They observe the tracer particles both near the mouth opening and in the distance of 400 μm from the protozoon. The maximal velocity in such system amounts

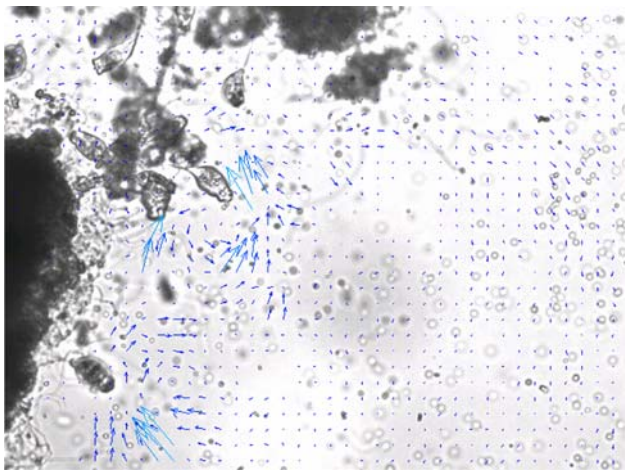

Fig. 1 Characteristic fluid flow situation observed during the experiments (the velocity field is depicted by *vector arrows*; see next section for details of the image generating and evaluating methods used)

up to 2,500 μm/s and is observed in the immediate close of cilia.

In comparison to Vorticella, smaller species, e.g. Epistylis cf. coronata indicate maximal velocities up to 180 μm/s. These investigations, where for detection of the fluid flow, small particles present in original samples are applied and are carried out by Fried and Lemmer (2003).

During ''standard'' feeding flow situation the microorganisms built the characteristic laminar vortex flow structure. Nevertheless, there are ciliate species that can destroy these patterns due to sudden contractions of the organism (Otto et al. 2001; Orme et al. 2003).

Species closely related to the sessile peritrichous ciliate *Opercularia asymmetrica* can be found in large amounts in bioreactors used in wastewater purification. Petermeier and Delgado (2006) and Petermeier et al. (2005, 2006) and Hartmann et al. (2006) analyse the fluid flow induced through these microorganisms using a biocompatible image generating flow visualisation for the first time. These authors aim at validating their work hypothesis which postulates the flow induced by the ciliates to be very efficient in transporting nutrients to the biofilm with minimal energy requirements. For ensuring, as high as possible, biocompatibility they not only adapt an invert microscope but also test the influence of biological appropriate seeding of different intensity and wavelength of the illumination as well as of open and closed microscope object holder. As most prominent results they find

- Three different scenarios of motion and rest.
- Pairs of motion eddies with a wave length which

corresponds to the distance between two neighbouring ciliates.
- Synergistically emphasised transport of nutrients by two ciliates which are intermittently active.

Figure 1 provides an impression of the flow field and also the seeding density with the biotic tracer particles.

Anyway, the detailed knowledge about such transport phenomena should contribute to a better understanding of biological processes. Additionally, it can be considered as a basis for the developing of technical solutions (bio-micromachines), which aim at, e.g. mixing of high viscous substances in microscale. Therefore, the current contribution intends further experimental and theoretical investigations of the fluid flow induced by ciliates. In agreement with earlier works (Petermeier and Delgado 2006; Petermeier et al. 2005, 2006; Hartmann et al. 2006), especially the biocompatibility of the applied optical measurement techniques is taken into account. However, the focus of the present contribution is on the management of the experimental data with the help of two different novel approaches:

(i) Neuronumerical hybrid in order to improve the data extracted from the particle image velocimetry (PIV) analysis and to detect artefacts.
(ii) Nonlinear optical filtering technique to improve the determination of the flow field.

2 Methods

2.1 Experimental methods

2.1.1 Microscopic particle-image-velocimetry

Opercularia asymmetrica has been selected from a laboratory Sequencing Batch Reactor (SBR). Further, probes with ciliates are prepared on microscope object holder consisting of glass plates both with and without cover plates. In the samples with cover plates the distance between the glass plates is set on 200 and 300 μm. Moving microorganisms and the induced fluid flow are observed with a microscope Axiovert S100 (Carl Zeiss, Germany) A 10-, 20- and 40-fold optical magnification is chosen due to requirements for good quality of image processing with PIV. PIV requires the selection of a cross section through the flow volume, in which the fluid flow is visualised through light scattering on suspended particles. The standard technique of a light sheet illumination is not applied here, since the intensity of the laser light confined to a very thin light sheet could disturb the natural behaviour of the organisms (see Hartmann et al. 2006). Therefore, the complete observation volume is illuminated in the present approach with a standard light source integrated in the microscope. The selection of the measurement plane is performed through focusing onto the desired plane of interest. The depth of the focusing plane does not exceed 10 μm.

In order to visualise the flow field induced by the ciliary movement of the organisms, flow tracers are injected with a pipette into the domain of observation. Cells of the yeast *Saccharomyces cerevisiae* (approx. 10 μm) are used as tracers. In contrast to conventional PIV, ordinary non-biological particles (polystyrene particles of 4.8 μm diameter from Microparticles GmbH, Germany) have been shown to be not suitable as they appear to be detected (most possible by chemotaxis) and rejected by the ciliates (Hartmann et al. 2006). Actually, the observed organisms reject the synthetic flow tracers as soon as they reach the vicinity of the mouth field. The rejection is generally of such strong intensity that the flow induced for transporting nutrients to the biofilm is strongly disturbed. In contrast, yeast cells (*S. cerevisiae*) are not rejected and their motion appears much smoother. In some cases, Opercularia ingested the yeast cells giving a first hint that latter may be appropriate as biological flow tracers. This points out that use of synthetic tracer particles is a direct intervention in the environmental conditions of the studied ciliates affecting their generic behaviour. Biological flow tracers reduce this source of error and can therefore be called biocompatible.

A critical issue in using flow tracers is the question whether those really follow the fluid flow or whether they deviate from the path lines due to inertial and viscous flow. For yeast cells, the analysis of the tracing properties carried out by Hartmann et al. (2006) confirms best traceability of these biological traces for such micro-flow applications.

Image sequences from CCD camera (MIKROTRON GmbH) with a macro-zoom objective allowing a maximum speed of 500 frames/s are recorded on the computer. Obtained frames have a resolution of 860 × 1,024 pixels (i.e. 602 μm × 505 μm).

PIV is carried out with the PIVview2C (PIVTEC GmbH), developed by Raffel et al. (1998). PIV needs image pairs of the measurement plane. In these image pairs, suspended flow tracers in sufficient quantity are observed. From the displacement of the tracers from one image to the next and the time interval between both images, two components of the velocity vector can be obtained (Adrian 1991). The association of tracers from one image to the next is carried out with statis-

tical correlation algorithms. The frames are interrogated with a Fast Fourier Transform accelerated interrogation algorithm. The interrogation window size is 32 × 32 pixels and the interrogation grid is 16 × 16 pixels. Figure 2 shows a part of Opercularia colony with distributed flow tracers.

In order to improve the biocompatibility of measurement systems other methods which require less intensity of illumination are tested. From reports in literature it was supposed that fluorescent tracers could facilitate measurements with low illumination intensity. Thus, colonies of *E. coli* marked with green fluorescence protein (GFP) have been used for flow field visualisation. Unfortunately, these experiments could not be finished successfully due to very high sensibility of employed species on changes of the environment. Nevertheless, this approach appears to be basically suitable for other organisms more robust to the stress produced by the illumination. Thus, further results will be published elsewhere.

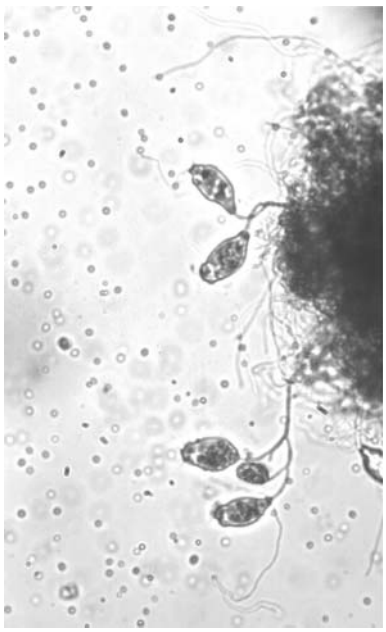

Fig. 2 Opercularia with distributed biotic tracers

In the next section, a different approach to obtain flow information in microscopic flow fields in vivo without using tracers and being directly applicable to phase objects is described, which fulfils the essential requirement of biocompatibility due to its very low laser power requirements. Furthermore, it contributes to the image generation by emphasising contrasts and removing quiescent background elements at the same time.

2.1.2 *Photorefractive novelty filter microscope (NFM)*

The photorefractive based optical novelty filter (Anderson and Feinberg 1989; Anderson et al. 1987) has been known for almost two decades. It is a temporal high pass filter (Anderson and Feinberg 1989; Anderson et al. 1987) which detects only the dynamic portions in the field of view while suppressing the quiescent background. Figure 3 shows a sketch of the experimental implementation of a novelty filter microscope (NFM), which is discussed subsequently in detail.

The most important highlight of this optical filter is that it is not only sensitive to amplitude changes but also to phase changes (Sedlatschek et al. 1999). Krishnamachari and Denz (2003, 2005) demonstrated that the phase sensitivity of the device can be used to detect and measure the phase changes in real time introduced by moving phase objects with an accuracy of $\lambda/20$, using light of the wavelength λ. In combination with a phase triggering technique (Krishnamachari et al. 2004) it is even possible to extend the phase

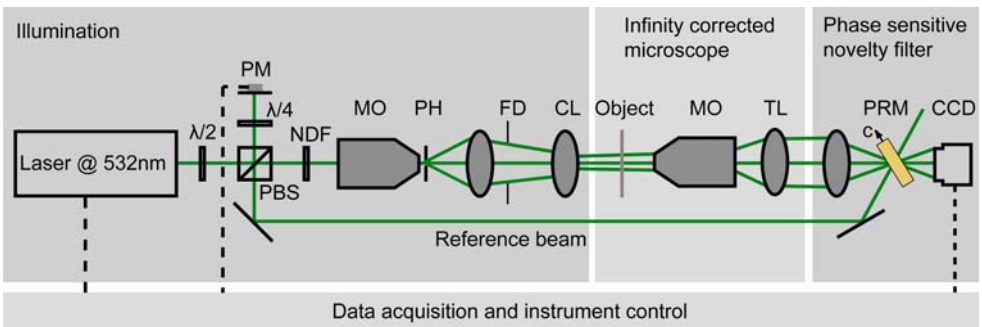

Fig. 3 Sketch of a novelty filter microscope setup. The setup can be divided into three main parts: illumination, microscope and novelty filter. *PM* piezo mirror, $\lambda/2$ half-wave plate, $\lambda/4$ quarter wave plate, *PBS* polarising beam splitter, *NDF* neutral density filter, *MO* microscope objective, *PH* pinhole, *FD* field diaphragm, *CL* condenser lens, *TL* tube lens, *c* optical axis, *PRM* photorefractive $BaTiO_3$ crystal, *CCD* camera

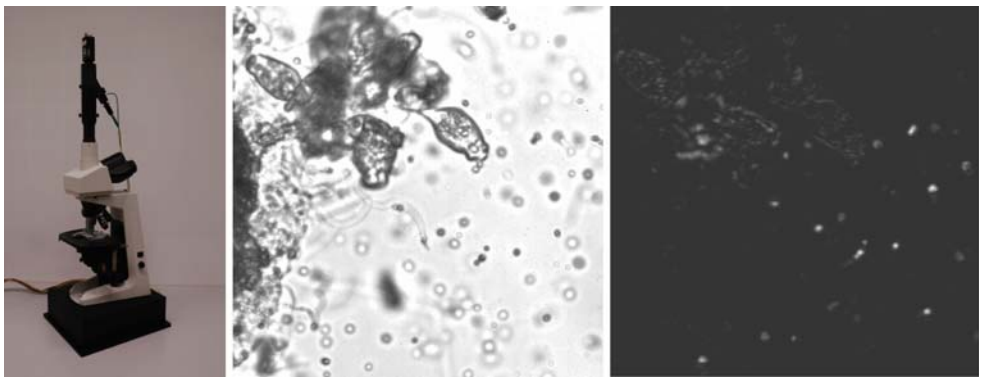

Fig. 4 Novelty filtering. *Left*: Application system NFM. *Middle*: Original image. *Right*: Same image scene after optical novelty filtering with the NFM

measurement range to 2π radians and to utilise the system for measuring concentration gradients in micro- and macro-mixing devices in real-time with a smallest measurable density change of 2.2×10^{-4} g/cm^3 (Krishnamachari et al. 2005; Holtmann et al. 2006a). In microbiological fields objects are often transparent and are thus phase objects. Hence the novelty filter can be used to get images of these moving objects with an increased contrast in comparison to conventional or phase contrast microscopy. Because of the low intensities of only nanowatts needed for novelty filtering, thus being biocompatible, the method can be used for long time observations of biological samples (Holtmann et al. 2006b).

Figure 3 shows the sketch of the experimental implementation of a NFM. A laser beam of wavelength 532 nm derived from a frequency-doubled Nd: YAG laser is split into a signal and a reference beam. The signal beam enters a conventional microscope and illuminates the object. The microscope objective and a projecting lens system produce a magnified image of the probe at the CCD camera. The images captured by the CCD camera are transferred to a PC for further analysis. The reference beam is made to interfere with the signal beam in a Ce-doped photorefractive $BaTiO_3$ crystal. The orientation of the *c*-axis of the crystal leads to a transfer of energy from the signal beam to the reference beam. This energy transfer results in a complete depletion of a static signal beam. Changes in the signal are not depleted thus being observed on the camera instantaneously. The power of the reference beam is 7 μW and that of the signal beam is about 300 nW. The relaxation time or the time constant for the grating build-up in the crystal is about 20 s. The choice of this large time constant helps to suppress trail formation and thus allows one-to-one imaging of moving objects in real-time (Krishnamachari and Denz 2003).

Figure 4 (on the left) shows a photograph of a novelty filter, implemented in a commercial microscope. Figure 4 (in the middle and on the right) gives an impression of the effect the NFM has on image sequences. The illustration in the middle shows a snapshot of the fluid flow, the illustration to the right depicts the result of NFM applied to the image sequence. Obviously, all static background information, like the biofilm on which the ciliate grows or the stationary ciliates zooid, is suppressed by the NFM. The more novelty a pixel represents, the brighter it appears in the NFM filtered image. Thus in the presented scene it can, e.g. be concluded that the ciliates (light grey shade) move slowly, whereas the bright spots give the positions of moving particles.

The novelty filter microscope (NFM) increases the contrast of amplitude and phase objects as a really non-invasive microscope technique. This allows three main advantages of images acquired with a NFM in microfluidics. At first it can be used in tracer based velocimetry (PIV) as a tool for capturing particle images with an increased signal to noise ratio compared to conventional or phase contrast microscopy (Holtmann et al. 2006b).

Secondly, it can be used to measure the velocity of particles using only a single captured image by using the trail formation of the optical novelty filter. And thirdly, the capability to measure phase changes in the field of view allows the determination of even small density or concentration changes in microfluidic flows in real time without the use of tracer particles or dyes (Krishnamachari et al. 2005). These features make the novelty filter microscope a powerful tool for investigation of microfluidic processes in bioinduced flows and online monitoring of processes in lab-on-a-chip devices. In this work the optical novelty filter is just used as a postprocessing method of digitally captured images for highlighting motions of tracer particles and microorganisms and can therefore not use the inherent features discussed before. Nevertheless, the capability of suppressing the static background and therefore increasing the contrast of the images is useful to test

the behaviour of the neuronumerical hybrid in combination with high contrast images and for a prefiltering process to deplete image artefacts.

2.2 Neuronumerical hybrid implementing the a priori knowledge formulated by the Taylor's hypothesis

In earlier works hybrid methods have been shown to be very powerful means in modeling, diagnosing and predicting complex systems (Delgado et al. 1996; Benning et al. 2001; Petermeier et al. 2002; Díez et al. 2006). Here a synergistic use of numerical flow simulation and artificial neuronal networks (ANN) is applied for detecting and correcting erroneous image artefacts automatically, which occur during the processing of PIV data. For this, a priori knowledge of the physics of the flow field is implemented into the hybrid in order to support the prediction performed by the ANN. The investigations carried out considered very different mathematical models for the implementation of a priori knowledge: the Bernoulli equation which assumed a potential flow, the Taylor's hypothesis adapted to flows dominated by viscous effects, the Stokes equation represented by an analytical Stokeslet solution of the Stokes equation given by Blake and Otto (1996) (see also Petermeier and Delgado 2006; Petermeier et al. 2005, 2006) and even the Navier–Stokes equations. For convenience, the present contribution focuses on the approach based on the Taylor's hypothesis. It represents a reasonable compromise between the numerical efforts to be done for supporting the ANN and the quality of their prediction. Furthermore, it appears to be in excellent agreement with the requirement in flow evaluation that the time allowed for detecting and correcting erroneous artefacts should be as short as possible.

The implementation of the Taylor's hypothesis into the ANN is done following the suggestion of Fellner et al. (2003), who created the so called ''functional nodes'' for emphasising the quality of the prediction of ANN. Figure 5 shows the working principle of such a neuronumerical hybrid based on a feed-forward neural network with one functional node.

The input layer feeds the independent variables to the network. Within a node the products of the output of the precedent nodes and the weights of the connections are summed up, i.e. $n_i = \sum_{p \in P} a(n_p) w_{pi}$. Here $a(n_p)$ calculates the activation of the precedent node n_p. The activation functions are sigmoid shaped functions. The weighted connections in the hidden layers propagate the calculation forward through the net to

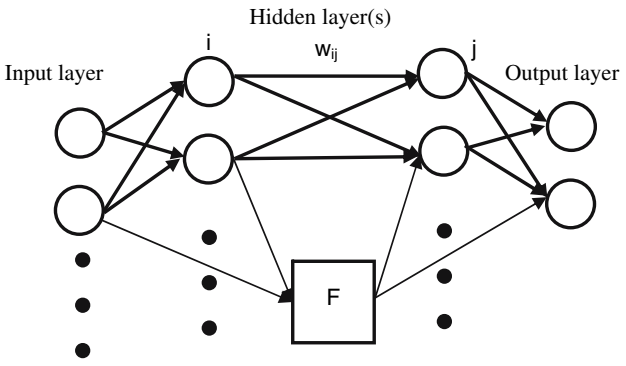

Fig. 5 Sketch of a feed forward neural network. The *circles* represent classical nodes (neurons), the *square* a functional node. The weights are represented by w_{ij} weighing the connection between nodes *i* and *j*

the output layer. During the training for each input vector the according output pattern $\vec{y}_i$ is confronted to the expected training pattern $\vec{t}_i$, in the case study, e.g. the velocity vectors obtained by a correlation based PIV algorithm (see Raffel et al. 1998). The error $\varepsilon = G\left(\left\|\vec{t}_i - \vec{y}_i\right\|\right)$ is calculated in a suitable norm, basically with the option to modify it with a quality function, which allows the introduction of additional penalty terms. The parameters of the map, i.e. the weights w_{ij}, are modified with the backpropagation algorithm, a gradient method, subsequently. The training is stopped when the training error falls below a prescribed bound (convergence).

Thus, artificial neural networks are a kind of approximators and especially this property makes a lot of appliances feasible. But a trained network represents a black-box model. For this reason knowledge extraction, and integration, is hardly possible. But, as shown by Fellner et al. (2003), functional nodes help to overcome this restriction, since with this approach the nodes in the involved layers can be labeled with a physical meaning and thus a priori knowledge can be integrated into such networks.

The functional node F in Fig. 6 specifies the a priori knowledge provided by the Taylor's hypothesis (Taylor 1938). The latter allows an interpretation of the physics of the flow in two totally different ways. It can be considered as a pure kinematic equation which expressed identical absolute values of the local acceleration and the convective acceleration. Classically, this is connected to the interpretation that ''frozen'' fluid particles move spatially with the time acceleration available at the point considered.

Note that the used training algorithm in the present case is the standard backpropagation algorithm. The classic ANN part is connected with the functional node part of the network using weights with the constant

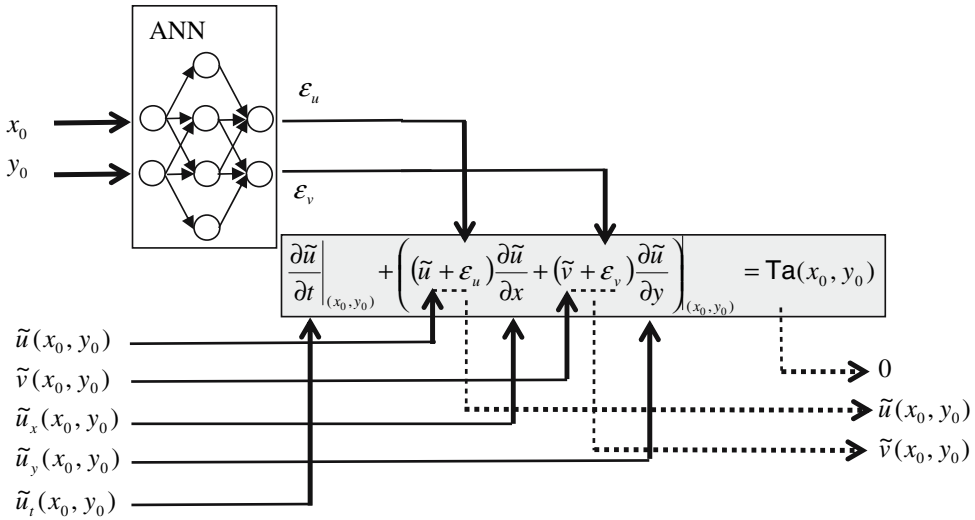

Fig. 6 Sketch of the used net configuration. The values with a tilde stand for the input or training data respectively. The *thick arrows* stand for the connections within the network with the constant weight *1*, i.e. these are edges excluded from the training. The trainable weights are in the part of the net symbolised by the box with the label "ANN". The *light grey* part symbolises the functional node. The *dotted lines* represent the edges with constant weights to the output layer

value 1, so they are excluded from the training but propagate the error back to the classic ANN part to minimise the sum squared error.

But additionally, this also holds for creeping flows as induced by microorganisms. Now, in such flows not only the effects of inertia can be neglected but also the outer forces such due to pressure, friction and mass forces are in balance, i.e. also dynamical restrictions are available. As a consequence of this, a hybrid based on the Taylor's hypothesis has impact on any prediction of the ANN which deviates from these kinematic or dynamic *a priori* conditions.

In the sense of the neuronumerical hybrid suggested for a velocity component, e. g. the x-component, the following expression can be derived from the Taylor's hypothesis:

$$\left.\frac{\partial \tilde{u}}{\partial t}\right|_{(x_0,y_0)} + \left.\left((u+\varepsilon_u)\frac{\partial \tilde{u}}{\partial x} + (v+\varepsilon_v)\frac{\partial \tilde{u}}{\partial y}\right)\right|_{(x_0,y_0)} = Ta(x_0,y_0). \tag{1}$$

Here the choice of one component is no restriction because of the coupling of the velocity components by the continuity equation for a pure incompressible fluid $\mathrm{div}\,\vec{v} = 0$.

In Eq. 1 (ε_u, ε_v) represent the velocity field corrections. The temporal derivative $\left.\frac{\partial \tilde{u}}{\partial t}\right|_{(x_0,y_0)}$ as well as the spatial $\left.\frac{\partial \tilde{u}}{\partial x}\right|_{(x_0,y_0)}$ and $\left.\frac{\partial \tilde{u}}{\partial y}\right|_{(x_0,y_0)}$ and the velocity field $(\tilde{u},\tilde{v})$ obtained, e.g. from the PIV evaluation is used as training input. Of course, in a preprocessing step the temporal and spatial derivatives must be calculated using an appropriate difference scheme from the velocity field $(\tilde{u},\tilde{v})$. The output vector for each training pattern consists of a scalar $Ta(x_0, y_0)$ denoting the degree of satisfaction of the Taylor's hypothesis which should be zero if the assumption holds for the corresponding velocity vector components $(\tilde{u},\tilde{v})$. So the correction velocity field (ε_u, ε_v) depending on the position is part of the artificial neural network. In contrast to this, the functional node is fed with $\tilde{u},\tilde{v},\tilde{u}_t,\tilde{u}_x,\tilde{u}_y,\varepsilon_u,\varepsilon_v$ as input. Consequently, the fulfilment of the Taylor's hypothesis is checked. Hereby, a comparison of the smoothened velocity field $(\tilde{u}+\varepsilon_u,\tilde{v}+\varepsilon_v)$ with the experimentally obtained velocity $(\tilde{u},\tilde{v})$ field is computed using $\varepsilon^2 = (\varepsilon_u)^2 + (\varepsilon_v)^2 + (Ta)^2$ as an estimator of the error. Since the training error is dominated by the areas where the Taylor's hypothesis is not valid, not only image analysis artefacts but also time-varying boundary conditions can be detected as it is shown in Fig. 8. Thus, the neuronumerical hybrid shows a twofold benefit: the removal of spurious vectors with the help of the correction velocity field as well as the detection of moving boundary.

Although these findings prove the synergistic use of image processing by PIV/PTV and the Taylor hybrid as an excellent method for determining the microorganismic flow field generated by ciliates, further methodological improvements are to be expected by implementing novelty filtering and model based visualisation.

In the current investigations the artificial neural network consists of one input layer with seven nodes (x and y coordinates, two velocity components, one temporal and two spatial derivatives of velocity), three hidden layers with ten nodes, one output layer with three nodes (two velocity components and Taylor value) and one functional node (see Eq. 1).

3 Presentation and discussion of results

Artefacts can be caused by lower quality of the image generation and acquisition or/and incorrect evaluation of the PIV images. As discussed above, in the case of microorganismic flows the number of measures possible for optimising the image generation and acquisition is strongly restricted by biocompatibility. Thus, they must be considered as the main source for artefacts. Of course, erroneous artefacts can also occur during the evaluation procedure of the PIV images.

Consequently, the neuronumerical hybrid is applied on the data provided by the correlation algorithm employed for the PIV evaluation. In order to generalise the statement regarding the action of the hybrid not only the PIV data obtained directly from the experiments are studied but also such which are ''randomly perturbed''. This should allow deriving statements for ''similar artefacts'' which can occur, e.g. when certain differences in the whole experimental data management take place.

Also, a comparison of the efficiency of the neuronumerical hybrid for treating data provided directly by the microscopic PIV and those by optical non-linear filtering is discussed.

However, the second benefit of the neuronumerical hybrid mentioned above is discussed first for convenience. In this case the hybrid delivers additional information on the existence of moving boundary conditions as available when a ciliate contracts itself.

3.1 Fluid flow perturbation induced by contractions of microorganisms

As a first test case for the Taylor hybrid a pair of pictures is selected, in which, in addition to the fluid flow provoked purely by the movement of the cilias, a contraction of the body (zooid) can be seen (e.g. Fig. 8). As discussed above the Taylor's hypothesis considers both spatial and temporal acceleration and thus the temporal velocity changes in a fixed point of the fluid flow can be transferred to spatial gradients.

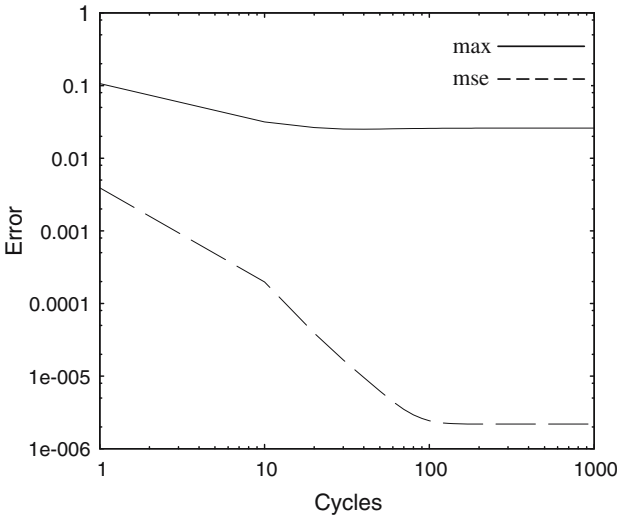

Fig. 7 Development of the maximal (max) and mean square error (mse) during the first 1,000 training cycles

The contraction movement of the microorganism represents a suddenly moving wall for the flow. Although for the form of the interaction of the water and the (soft and flexible) zooid no fluid mechanical description has been given in literature, yet it induces significant perturbations in the basic two dimensional velocity field consisting of pair of eddies generated by the pure movement of the cilia, see Fig. 1 and compare Blake and Otto (1996).

Such phenomena can be observed not only optically but are also represented during the training phase of the hybrid, see Fig. 7. Analysing the training error in Fig. 7, ($\max = \max_i \left(\left\| \vec{t}_i - \vec{y}_i \right\|_2 \right)$ and $\text{mse} = \frac{1}{N} \sum_i \left\| \vec{t}_i - \vec{y}_i \right\|_2$) it can be seen that after a relatively

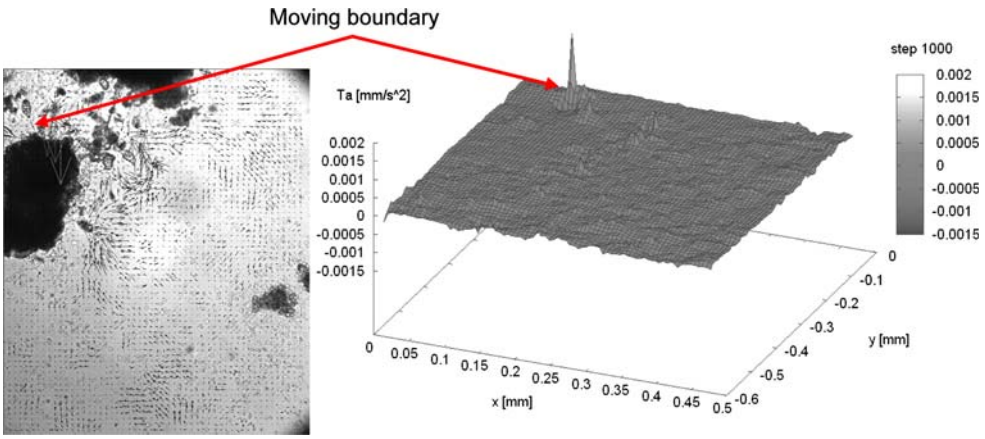

Fig. 8 Fluid flow situation with the detected moving boundary

small number of approximately 100 steps the training errors reach a plateau.

The comparison of this curve development with two-dimensional distribution of the training error illustrated in Fig. 8 shows that the error reached at the beginning of learning is located in the places of highest velocities, so in the vicinity of the active ciliate. In the next stage the error decreases and after 150 steps it is finally dominated by the fluid motion caused by contracted Opercularia. Figure 8 visualises the training error distribution after 1,000 training cycles. The contraction which corresponds, from the fluid mechanical point of view, to a suddenly moved (soft and flexible) wall is depicted graphically as a peak with the maximum training error. This documents the ability of the employed neuronumerical hybrids to detect and remove flow incidents which deviate from the flow patterns learned by the ANN and the physical knowledge implemented a priori.

One training step (processing of 3,275 data sets for flow field estimation, backpropagation and update) with the used net built of 50 nodes takes about 3.5 ms, the complete run for the 1,000 cycles takes about 20 min on an AMD Athlon 64 Processor with JAVA 1.5.0 virtual machine.

3.2 The action of the Taylor hybrid on PIV data superposed by artificial noise

As mentioned above, to assess the effectiveness of the presented Taylor hybrid approach, the experimentally acquired and evaluated flow field was manipulated artificially. Hereby, random noise disturbs the randomly chosen velocity vectors of the evaluated PIV data. In order to be able to distinguish between the detection and correction abilities of the neuronumerical hybrid, the image sequence with the contracting ciliate is selected. For the data preparation, two subsequent velocity fields obtained with the correlation based PIV are selected. The disturbance of the velocity vectors is applied by multiplying their absolute values with random numbers from the interval [-5;5]. Then the modified velocity fields are processed to get the necessary derivatives with respect to time and space as training data. Since the number of spurious velocity vectors cannot be estimated in advance, the influence on the artefact detection and flow field reconstruction is studied using ten randomly manipulated vectors (denoted as P1...P10 in Figs. 9, 10) out of 3,276.

The influence of the randomly applied artificial noise on the training progress is shown in Figs. 9 and 10. Figure 9 visualises the relative error $\frac{|\vec{V}_{\text{noise}}|-|\vec{V}_0|}{|\vec{V}_0|}$ in percent, where $|\vec{V}_0|$ is the absolute value of the undisturbed velocity vector of the evaluated PIV data and $|\vec{V}_{\text{noise}}|$ is the absolute value of the corresponding velocity vector including noise. Apparently, the absolute value of the ratio decreases towards zero. This means that the artificial errors are detected correctly and the countermeasures proposed automatically by the hybrid are also accurate.

Concerning the angular difference, which is depicted in Fig. 10, the tendency to correct the errors can be observed but is not carried out to such an extent as illustrated in Fig. 9. The reason, which will also be discussed later, is that due to the training data preparation, some of the ''angular information'' for the velocity vector is lost.

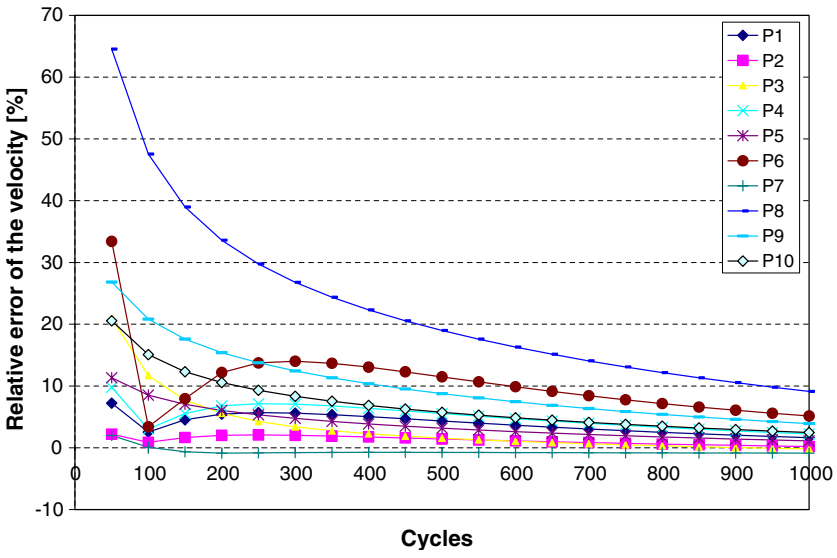

Fig. 9 Relative error of the velocity in the ten points (P1...P10) altered randomly. The data provided by the PIV evaluation are compared with the data after the correction with the neuronumerical hybrid

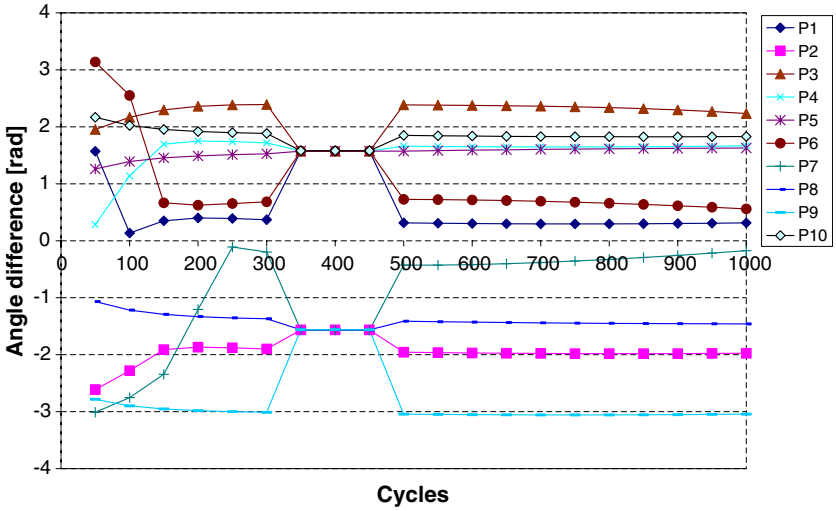

Fig. 10 The angle difference between the velocity vector of raw PIV data after the correction with the neuronumerical hybrid

3.3 Visualisation of velocity distribution with and without optical novelty filtering (ONF)

The fluid flow situation shown in Fig. 11 is also analysed with the neuronmerical hybrid based on the Taylor's hypothesis. In this experiment the images without and with ONF are analysed. To get an impression on the flow situation, the tracer particle paths are visualised by image superposition, see Fig. 11. It can be seen that the pathlines, in the present case due to the underlying Stokes flow regime as well as the streamlines, are identical.

This illustrates the capability of ONF to provide reliable information although the intensity of the illumination required is only a small part of that necessary for the direct microscopic PIV. In this context, it must be pointed out that the optical novelty filtering was carried out using digital images, i.e. a case for which the ONF is not originally developed for and thus cannot show its full abilities. Nonetheless, this "post" optical novelty filtering highlights imaging artefacts of the original obtained images, which are not known and cannot be quantified a priori. These highlighted artefacts can be detected and, to a certain extent, corrected by the neuronumerical hybrid as it is discussed in the following.

For both image sequences a PIV analysis was carried out. The resulting velocity fields were identically preprocessed for training data usage in the neuronumerical hybrid. The standard backpropagation algorithm (see, for example Rojas 1996) with fixed stepsize was used as training algorithm to avoid additional influences during the training. Additionally, preliminary studies have shown that training algorithms with stepsize control did not improve the convergence speed. Figure 12 summarises the results obtained by training. Obviously, the application of the neurohybrid automatically corrects the velocities. From the results of the application of the Taylor hybrid on the data with artificial noise, it is obvious that the correction is of beneficial effect.

In the present case it can be observed that the Taylor term converges towards zero in the whole region of interest. Thus, the neural network part of the hybrid learns correctly the correction velocity field (ε_u, ε_v).

Regarding the convergence velocity, the case with the spurious vectors did neither converge as fast as the

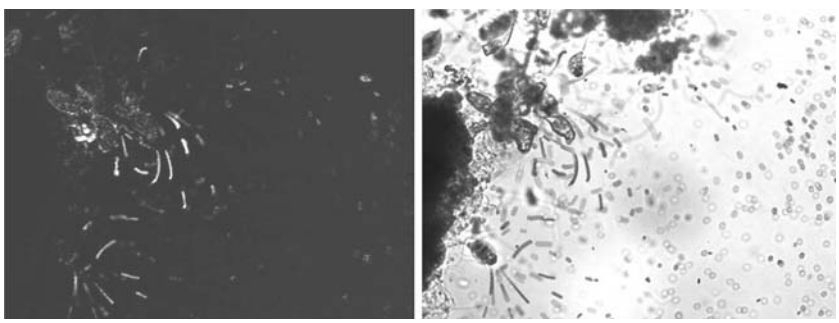

Fig. 11 Illustration of the analysed flow situation by pathlines generated using image superposition. *Left*: Optical novelty filtering. *Right*: Unfiltered images

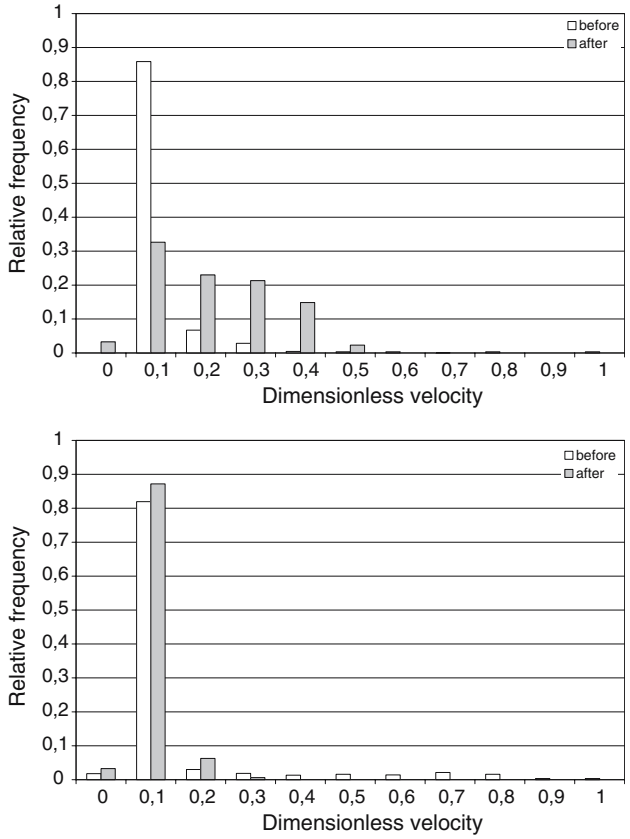

Fig. 12 Relative frequency for the 1,131 of the velocity vectors ratio without (up) and with optical novelty filtering (down) versus the dimensionless velocity (for the reference velocity the maximal velocity from the flow field is taken). The *white columns* refer to before, the *grey columns* after the treatment with the Taylor hybrid

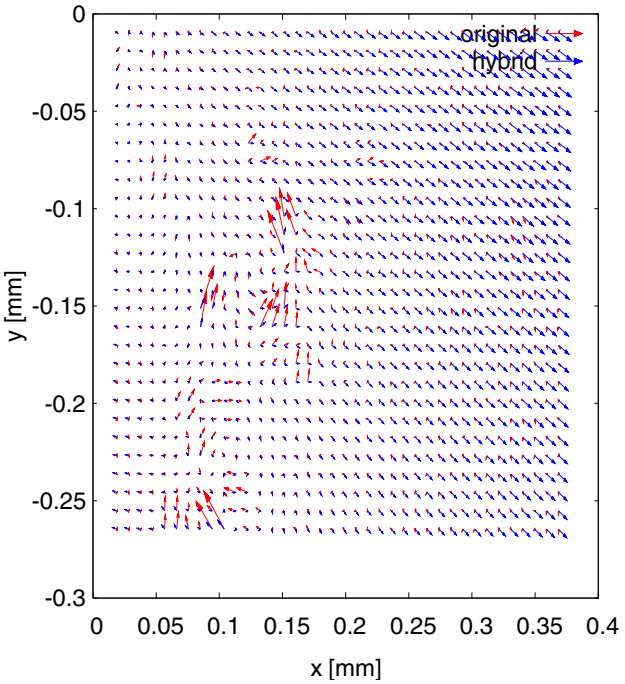

Fig. 13 PIV-velocity field before (*black arrows*) and after (*grey arrows*) the application of 1,000 cycles training of the Taylor hybrid

training with undisturbed velocity vectors nor did it reach the same convergence level. One reason is that the strong excess of the spurious vectors contributes overproportionally to the training error. Further, the Taylor term serves as a detector for spurious vectors, whereas for a higher number of training cycles the weight adaptation leads mainly to a decrease of the Taylor term towards zero.

Figure 13 exemplifies the effect of the Taylor hybrid applied on the PIV velocity fields obtained from the unfiltered images.

To overcome the limitations, an adaptive stepsize control could be beneficial. In this case it should be taken into consideration that the classic strategy for stepsize control in the backpropagation algorithm does not take into account the partial derivatives with respect to time and space. But exactly this is of great importance for a successful convergence of the training and can be motivated by the stepsize control schemes used in the computational fluid dynamics.

Overall, it can be concluded that the presented approach is suitable for the detection of image and automatic correction of artefacts. But the correction abilities have potential for further development. Possibly, successful strategies are the use of cellular neural networks (CNN- Liang et al. 2003) and a more specific determination of the angular orientation of the velocity field. The CNN are based on an equidistant grid and are thus able to incorporate algorithms, which are commonly used in the computational fluid dynamics, e.g. information on the boundary.

As yet, the influence of the angular orientation is suppressed due to the classical preparation of the training data. Splitting of the velocity vector in a base (in Cartesian coordinates) indicating the positions of the PIV-grid and a polar notation describing precisely the vector direction, i.e. absolute value and angle, can overcome this.

4 Conclusions

This paper presents a novel neuronumerical hybrid for the detection and automatic correction of artefacts. It is based on the implementation of numerically expressed a priory knowledge on the flow field (Taylor's hypothesis) into an artificial neural network as a

functional node. The proper functionality of the neuronumerical hybrid is demonstrated as an example from microfluidics which occurs when biocompatible image generating techniques are applied for studying microorganismic convection induced by ciliates. The neuronumerical hybrid has been proven to detect reliably the spurious velocity vectors provoked by both image artefacts and moving boundaries like the contraction of the zooid, as shown in the example.

The non-linear optical novelty filtering offers additional advantages due to the enhancement in contrast and the removing of quiescent objects. To be more precise, due to the ONF working as a temporal high pass filter, all time-independent information such as the background is blocked instantaneously. Furthermore, and for the case of the microorganismic induced flow of great advantage, the use of the ONF allows an extended observation time while strictly keeping the necessary biocompatibility. Despite the strong nonlinearity of the ONF, the same neuronumerical hybrid could also serve as artefact detector.

Thus, the Taylor's hypothesis is suitable to correct and improve the experimentally obtained flow fields. Further work will be dedicated to the enhancement of the presented approach with the goal to speed up convergence and to allow an even more precise reconstruction of the flow field. Last but not the least, it must be stated that the neuronumerical hybrid is successful in dealing with images of extremely poor quality as further improvements are not compatible with the biocompatibility that is basically required in the considered microorganismic flow. Thus, it is expected to be even more efficient in suppressing artificial artefacts in other flow cases in which an optimisation of the image generating process is more easily possible. Of course, ONF can contribute additionally to the improvement of images due to its highly powerful filtering ability.

Acknowledgments This study was supported by the German Research Foundation (DFG), projects DE 643/10-1, DE 643/10-2 and DE 486/14-2.

References

Adrian RJ (1991) Particle-image techniques for experimental fluid mechanics. Ann Rev Fluid Mech 23:261–304

Anderson DZ, Feinberg J (1989) Optical novelty filters. IEEE J Quantum Electron 25:635–647

Anderson DZ, Lininger DM and Feinberg J (1987) Optical tracking novelty filter. Opt Lett 12:123–125

Benning R, Becker T, Delgado A (2001) Initial studies of predicting flow fields with an ANN hybrid. Adv Eng Softw 32:895–901

Blake JR, Otto SR (1996) Ciliary propulsion, chaotic filtration and a blinking stokeslet. J Eng Math 30:151–168

Delgado A, Nirschl H, Becker T (1996) First use of cognitive algorithms in investigations under compensated gravity. Micrograv Sci Technol IX(3):185–192

Díez L, Zima BE, Kowalczyk W, Delgado A (2006) Investigation of multiphase flow in Sequencing Batch Reactor (SBR) by means of hybrid methods. Chem Sci Eng (in press)

Eisenmann H, Letsiou I, Feuchtinger A, Beisker W, Mannweiler E, Hutzler P, Arnz P (2001) Interception of small particles by flocculent structures, sessile ciliates, and the basic layer of a wastewater biofilm. Appl Environ Microbiol 67:4286–4292

Fellner M, Delgado A, Becker T (2003) Functional neurons in dynamical neural networks for bioprocess modelling. Bioprocess Biosyst Eng 25:263–270

Foissner W, Berger H, Kohmann F (1992) Taxonomische und ökologische revision der Ciliaten des Saprobiensystems—band II: Peritrichia, Heterotrichida, Odontostomatida. Informationsberichte des Bayer. Landesamtes für Wasserwirtschaft, Heft 5/92, München

Fried J, Lemmer H, (2003) On the dynamics and function of ciliates in sequencing batch biofilm reactors (SBBR). Water Sci Technol 47: 189–196

van Ginneken V, Antonissen E, Müller UK, Booms R, Eding E, Verreth J, van den Thillart G (2005) Eel migration to the Sargasso: remarkably high swimming efficiency and low energy costs. J Exp Biol 208:1329–1335

Hartmann C, Özmutlu Ö, Petermeier H, Fried J, Delgado A (2006) Analysis of the flow field induced by the sessile peritrichous ciliate *Opercularia asymmetrica*. J Biomech (in press)

Holtmann F, Krishnamachari VV, Grothe O, Deitmar H, Eversloh M, Wördemann M, Denz C (2006a) Measurement of density changes in fluid flow by an optical nonlinear filtering technique. In: 12th International symposium on flow visualisation (ISFV 2006)

Holtmann F, Wördemann M, Eversloh M, Grothe O, Deitmar H, Krishnamachari VV, Denz C (2006b) Echtzeitbestimmung von Geschwindigkeits- und Dichtefeldern in Mikroströmungen mit Hilfe optisch nichtlinearer. In: Proceedings 14. GALA 2006, Braunschweig 5.-7.9.2006

Krishnamachari VV, Denz C (2003) Real-time phase measurement with a photorefractive novelty filter microscope. J Opt A Pure Appl Opt 5:239–243

Krishnamachari VV, Denz C (2004), A phase-triggering technique to extend the phase-measurement range of a photorefractive novelty filter microscope. Appl Phys B Lasers Opt 79:497–501

Krishnamachari VV, Grothe O, Deitmar H, Denz C (2005) Novelty filtering with a photorefractive lithium–niobate crystal. Appl Phys Lett 87:071105

Liang DF, Jiang CB, Li YL (2003) Cellular neural network to detect spurious vectors in PIV data. Exp Fluids 34:52–62

Orme BA, Blake JR, Otto SR (2003) Modelling the motion of particles around choanoflagellates. J Fluid Mech 475:333–355

Otto SR, Yannacopoulos AN, Blake JR (2001) Transport and mixing in Stokes flow: the effect of chaotic dynamics on the blinking stokeslet. J Fluid Mech 430:1–26

Petermeier H, Delgado A (2006) ANNalyzer basierend auf der Taylor-Hypothese zur Stützung eines Bildauswerteverfahrens für mikroorganismische Strömungen. In: Proceedings 14. GALA 2006, Braunschweig 5.-7.9.2006

Petermeier H, Benning R, Delgado A, Kulozik U, Hinrichs J, Becker T (2002) Hybrid model of the fouling process in tubular heat exchangers for the dairy industry. J Food Eng 55:9–17

Petermeier H, Baars A, Delgado A (2005) ''ANNalyzer''—neurohybride Stützung eines Bildauswerteverfahrens, angewendet auf mikroorganismisch generierte Strömungen. In: Proceedings 13. GALA 2005, S. 12.55-1-12.55-6, Cottbus 6.-8.9.2005

Petermeier H, Delgado A, Kondratieva P, Westermann R, Holtmann F, Krishnamachari V, Denz C (2006) Hybrid approach between experiment and evaluation for artefact detection and flow field reconstruction—a novel approach exemplified on microorganismic induced fluid flows. In: 12th International symposium on flow visualization (ISFV 2006) (in press)

Raffel M, Willert Ch E, Kompenhans J (1998) Particle image velocimetry. A practical guide. Springer, Berlin

Rojas R (1996) Neural networks—a systematic introduction. Springer, Berlin

Sedlatschek M, Trumpfheller J, Hartmann J, Müller M, Denz C, Tschudi T (1999) Differentiation and subtraction of amplitude and phase images using a photorefractive novelty filter. Appl Phys B Lasers Opt 68:1047–1054

Sleigh MA, Barlow D (1976) Collection of food by vorticella. Trans Am Micros Soc 95:482–486

Taylor GI (1938) The spectrum of turbulence. Proc R Soc Lond A 164:476–490